Catal Lett (2008) 124:185–194
DOI 10.1007/s10562-008-9500-y

Silica–Titania mixed Oxides: Si–O–Ti Connectivity, Coordination of Titanium, and Surface Acidic Properties

Jun Ren · Zhong Li · Shusen Liu · Yanling Xing · Kechang Xie

Received: 3 March 2008 / Accepted: 19 April 2008 / Published online: 1 May 2008

Abstract A series of SiO_2–TiO_2 mixed oxides was prepared by the sol–gel route, and the influence of several important preparation parameters (Ti precursors, content, and calcination temperature) on the Si–O–Ti connectivity, coordination of titanium and surface acidity has been studied using various analytical techniques. The solids obtained were largely amorphous and characterized by Ti enrichment on surfaces with low titanium content; however, the addition of titanium greater than 50 mol% into the SiO_2 matrix led to significant phase separation of crystalline anatase. The Ti atoms are tetrahedrally coordinated with Si/Ti ratios higher than 10 and gradually enter into octahedral positions in the silica matrix with further increase in the titanium content. High-temperature treatment can break Si–O–Ti linkages and eliminate hydroxyl groups, resulting in a decrease in acid site density.

Keywords SiO_2–TiO_2 mixed oxides · Si–O–Ti linkages · Titanium coordination · Tetrahedral Ti(IV) species · Silica matrix · Surface acidity

1 Introduction

Amorphous mixed silica–titania materials, whose properties depend on their composition, homogeneity and structure, have attracted considerable interest due to their potential applications as catalysts and supports in a wide variety of reactions [1]. It is evident that there is, in general, a positive correlation between catalytic performance and Si–O–Ti connectivity [2]. The use of the sol–gel route to prepare raw SiO_2–TiO_2 solids allows us to obtain materials with high homogeneity and good titanium dispersion, and to control their composition and properties [3]. A great variety of spectroscopic techniques have been used to gather information about the formation of Si–O–Ti linkages, the coordination geometry of the Ti atoms in the silica matrix as well as the strong interaction between silica and titania [4–12].

Compared to the bulk properties, however, relatively little is known about the surface properties of SiO_2–TiO_2 mixed oxides [13]. Previous studies have demonstrated that surface acidity of the material is vital to its catalytic behavior in many reactions, including epoxidation [14], isomerization [15], transesterification [16], nitration of toluene [17], catalytic combustion of volatile organic compounds (VOCs) [18], and selective catalytic reduction (SCR) reaction [19]. To comprehend the mechanism of their catalytic action, and predict their activity and selectivity, information is needed on the nature, amount and strength of the acid sites exposed on their surface. In general, pure titania only has Lewis acid properties whereas the silanol groups (Si–OH) of silica are so weakly acidic that the material is generally classified as inert. However, SiO_2–TiO_2 mixed oxides exhibit a large number of acidic sites and acid strength which depend on the metal oxide relative content, nature and method of preparation [20, 21]. The new acidic sites are assumed to be produced by charge imbalance localized at the Si–O–Ti bonds owing to the difference in coordination geometries of Si and Ti [22].

Structural features of SiO_2–TiO_2 mixed oxides and their relationship with the physicochemical and catalytic properties remain poorly understood due to the lack of

J. Ren (✉) · Z. Li · S. Liu · Y. Xing · K. Xie
Key Laboratory of Coal Science and Technology, Taiyuan University of Technology, Ministry of Education, No. 79 Yingze West Street, Taiyuan, Shanxi Province 030024, China
e-mail: renjun@tyut.edu.cn

systematic fundamental studies [23]. In contrast to the large number of studies carried out on the influence of surface acidity on catalytic activity, to our knowledge, research devoted to the correlation between the resulting surface acidity and the bulk properties (such as Si–O–Ti connectivity and coordination of titanium) is scanty in the literature. Although the importance of catalytic properties of SiO_2–TiO_2 mixed oxides has been emphasized by extensive characterization studies, the nature of the active site required to achieve high activity and selectivity is not well understood. On the other hand, a broad range of spectroscopic methods have been applied for structural characterization but the results are far less informative than in the case of well-defined, crystalline Ti-substituted zeolites [24]. It is commonly accepted that there is a limit to the proportion of Ti atoms that can be effectively incorporated into the zeolite framework [25]. For SiO_2–TiO_2 mixed oxides, however, the maximum titanium content that can enter by substitution into the silicon sites remains an important matter seldom discussed.

In this contribution, we report on the effect of preparation parameters (Ti precursors, content, and calcination temperature) on the structural and chemical properties of SiO_2–TiO_2 mixed oxides by using a combination of analytical techniques. The aim is to gain insight into the pertinent correlation between Si–O–Ti connectivity, Ti coordination and surface acidic properties of SiO_2–TiO_2 mixed oxides. With properly chosen experimental parameters, one can control the surface acidity of the material so as to meet the requirements of various catalytic reactions.

2 Experimental

2.1 Preparation of SiO_2–TiO_2 Mixed Oxides

The raw SiO_2–TiO_2 solids were prepared by co-gelation of silicon tetraethoxide (TEOS) with titanium tetraisopropoxide (TTIP) or titanium tetraethoxide (TEOT) as follows: two solutions consisting of (*A*) EtOH + TEOS + HAc + H_2O and (*B*) EtOH + TTIP (or TEOT) + HAc + H_2O were placed in separate beakers, where HAc was added to both solutions to enhance the hydrolysis process and allow a more compatible hydrolysis rate between TEOS and TTIP (or TEOT). Since TTIP and TEOT were hydrolyzed more rapidly than TEOS, this might lead to homocondensation of the Ti species, thus TEOS was pre-hydrolyzed for 1 h (solution *A*) and then mixed with solution *B*. The beaker containing the mixture of solution *A* and *B* was covered with parafilm and stored overnight with stirring until converted into a solid cogel. The cogel was first retained at room temperature for about 1 week to remove alcohols and water. The resultant xerogel was first heated in air at a rate of 0.5 °C/min from room temperature to 65 °C and held for 3 h and then with a similar heating rate to a higher temperature (250–650 °C) and held for another 4 h to eliminate the organic residues. To observe the effect of Ti content on the physical and chemical properties of SiO_2–TiO_2 mixed oxides, a series of cogels have been obtained by varying the Si/Ti ratios between 0.1 and 10 and presented by the general formula ST*x* (*x* = Si/Ti atomic ratio). Pure silica was also obtained for comparison.

2.2 Physico-chemical Characterization

X-ray diffraction (XRD) analysis was carried out using a D/max 2500 diffractometer (Rigaku, Japan), and the diffractograms were recorded with CuK_α radiation over a 2θ range of 10–80.

The Brunauer–Emett–Teller (BET) surface area (S_{BET}) and desorption pore volume (V_p) were evaluated by the Barrett–Joyner–Halenda (BJH) method and determined by N_2 physisorption at −196 °C using a SORPTMATIC 1990 instrument (CE, Italy). Before measurement, the sample was degassed at 120 °C until a final pressure below 0.1 Pa was achieved.

Thermal gravity analysis (TGA) investigation of selected xerogels was performed on a STA 409C thermogravimetric analyzer (Netzsch, Germany). The temperature was programmed to increase at a rate of 10 °C/min from room temperature to 800 °C under circulation of dried air.

Fourier transform infrared spectroscopy (FTIR) measurements were conducted on a FTS-165 spectrometer (Bio-Rad, USA) in the range 400–4000 cm^{-1} using KBr as the background. Each spectrum was recorded at 4 cm^{-1} resolution with 500 scans.

Pyridine-FTIR studies were carried out in a high-temperature flow infrared cell-reactor. The sample was previously calcined in an airflow at 300 °C for 1 h. After evacuation (1×10^{-6} Torr), pyridine mixture was introduced at a flow rate of 150 cm^3/min for 0.5 h. Then the cell reactor was cooled to 150 °C for 20 min to eliminate the excess pyridine. The FTIR spectra of adsorbed pyridine were recorded.

The UV–Vis diffuse reflectance spectra in the wavelength range of 200–800 nm were obtained on a Lambda Bio-40 spectrophotometer (PE, USA) at room temperature after prior heat treatment. Again, the samples were carefully protected from ambient moisture.

X-ray photoelectron spectroscopy (XPS) data were obtained with an ESCALab220i-XL electron spectrometer (VG, UK) using 300 W AlK_α radiation. The pressure of the analysis chamber was maintained at 3×10^{-9} mbar. The BE and the Auger kinetic energy (KE) scales were calibrated by setting the C 1 s transition at 284.6 eV. The BE

and KE values were obtained using the Peak-fit program implemented in the control software of the spectrometer.

Temperature-programmed desorption of ammonia (ammonia TPD) analysis was carried out in an AutoChem II 2920 apparatus (Micromeritics, USA) to estimate the amount and strength of acid sites. The sample was fluxed with a He flow at temperatures up to 500 °C, maintained for 1 h at this temperature, and then was allowed to cool down to room temperature and exposed to flowing NH_3 (15% in He) for 0.5 h. Afterwards, the system was purged for 0.5 h with helium to eliminate the excess NH_3 gas. The temperature of the sample was then raised linearly (10 °C/min) from room temperature to 600 °C. The desorbed NH_3 was monitored by means of a thermal conductivity detector and quantified by comparing the areas under the curve of the respective thermograms with those obtained from previous calibration using known amounts of NH_3.

3 Results and Discussion

3.1 Textural Properties

Pure silica and SiO_2–TiO_2 mixed oxides (Si/Ti = 1, 5, 10, 50) were obtained by thermal treatment of the xerogels in air at a final temperature of 550 °C as described in Sect. 2.1. The four compositions were carefully chosen to represent the region of distinct structural behavior in this system. Some of the textural property values are listed in Table 1. Pure silica displays a low BET surface area (107 m^2/g) and small pore volume (0.06 m^3/g). However, distinctly higher values are obtained in the case of SiO_2–TiO_2 mixed oxides. Furthermore, both BET surface area and pore specific volume gradually decrease with the increase in the titanium content of mixed oxides.

Figure 1 shows a typical nitrogen isotherm curve (Si/Ti = 10) as well as pore size distributions of pure silica and SiO_2–TiO_2 mixed oxides. It shows the type I + IV isotherm according to the Brunauer, Deming, Deming, and Teller (BDDB) classification with two very distinct regions: at very low relative pressure ($P/P_0 < 0.2$), the isotherm exhibits high adsorption, revealing the presence of micropores (type I). The isotherm shows a large type H2 (IUPAC classification) hysteresis loop at relative pressures (P/P_0) between 0.2 and 0.9, indicating that mesopores are also present in the mixed oxides [26]. Pure silica only has pores with a diameter smaller than 15 Å. However, SiO_2–TiO_2 mixed oxides display a striking increase in pores with these diameters compared with pure silica and also have pores with diameters of roughly 15–25 Å. It is noted that the ST10 sample appeared to show the minimum abundance of newly produced pores.

Table 1 BET surface areas and total pore volumes of pure silica and SiO_2–TiO_2 mixed oxides

Sample	X^a (mol %)	$S_{BET}{}^b$ (m^2/g)	V_p^c (m^3/g)
SiO_2	0	107	0.06
ST50	1.96	595	0.36
ST10	9.09	434	0.26
ST5	16.67	324	0.20
ST1	50.00	162	0.10

[a] Ti molar fraction: X = Ti/(Si + Ti) * 100

[b] BET surface area calculated from the linear part of the BET plot (P/P_0 = 0.05–0.30)

[c] Pore specific volume

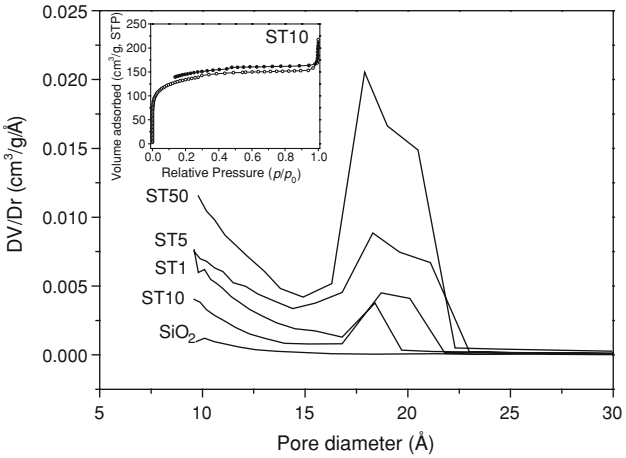

Fig. 1 Pore size distributions of pure silica and SiO_2–TiO_2 mixed oxides (5–30 nm)

3.2 Crystal Structure

The crystal structure of SiO_2–TiO_2 mixed oxides with different Si/Ti ratios has been studied in detail in the range from 0.1 to 10. The XRD patterns are shown in Fig. 2. The mixed oxides with Si/Ti ratios between 1 and 10 exhibit a broad diffraction peak within the 2θ range 10–40, characteristic of amorphous silica. This indicates that the titanium is highly dispersed in the silica matrix and does not exist as crystals of size sufficient to be detected by XRD. The diffraction peak is gradually shifted to higher 2θ angles with the increase in titanium content in the mixed oxides. One possible explanation is that distortion of the crystal structure of the SiO_2 matrix is caused by introduction of Ti species.

Since no diffraction peaks related to Ti species are observed, it can be considered that the Ti^{4+} ions may enter the SiO_2 network and take the place of some Si^{4+} ions, leading to a homogeneous distribution of isolated Ti^{4+} species in the silica matrix. It has been reported that the radius of Si^{4+} ions is 0.41 Å while it is 0.68 Å for Ti^{4+} ions,

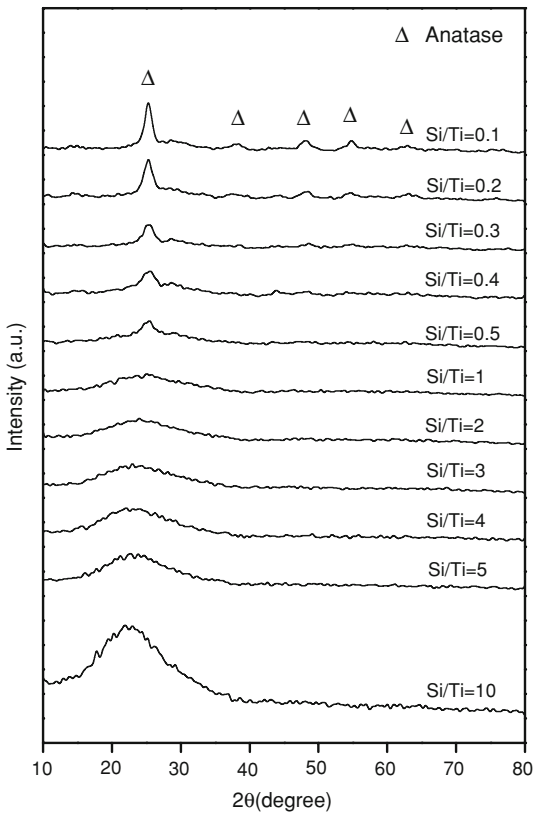

Fig. 2 XRD patterns of SiO_2–TiO_2 mixed oxides with various Si/Ti ratios

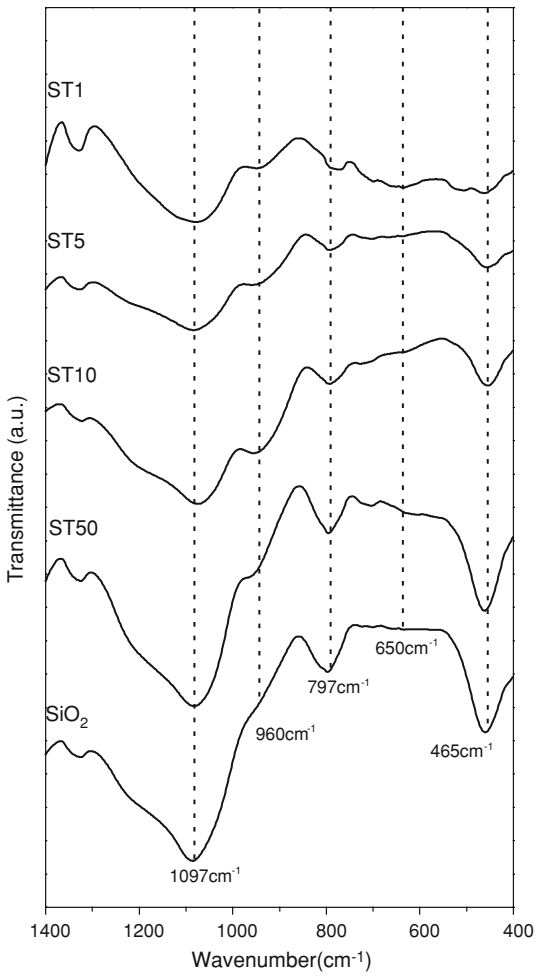

Fig. 3 FTIR spectra of pure silica and SiO_2–TiO_2 mixed oxides

so the substitution of Si^{4+} by larger tetrahedra of Ti^{4+} can cause some distortion in the SiO_2–TiO_2 network or in the silica-rich matrix. This change in crystal structure is therefore reflected in shifts in the diffraction peak positions [27]. In the case of mixed oxides with Si/Ti < 1, diffraction peaks corresponding to anatase crystals can be observed and increase slightly with an increase in titanium content, revealing the formation of crystalline titania. The present results, therefore, show that mixing of Si and Ti at an atomic level occurs in the sol–gel process, while higher amounts of Ti addition lead to segregation of TiO_2 particles.

3.3 Effect of Preparation Parameters on Si–O–Ti Connectivity

FTIR spectroscopy was used to gain information about the formation of Si–O–Ti linkages. FTIR spectra of pure silica and SiO_2–TiO_2 mixed oxides are shown in Fig. 3. The strong IR absorbances at 1097 and 797 cm^{-1} can be assigned to symmetric ν_s(Si–O–Si) stretching vibrations, and asymmetric ν_{as}(Si–O–Si) stretching vibrations, respectively [4]. The band at 465 cm^{-1} corresponds to Si–O–Si bending modes. The band at 960 cm^{-1} is usually coupled with the hint of tetrahedral coordination of Ti^{4+} ions which should substitute for Si^{4+} ions in the bulk matrix of SiO_2–TiO_2 mixed oxides with low titanium content [28].

Pure silica shows no absorption signal around 960 cm^{-1}. However, the 960 cm^{-1} band is clearly detected in the case of SiO_2–TiO_2 mixed oxides, indicating the presence of Si–O–Ti linkages. The remarkable decrease in the 465 cm^{-1} band with increasing titanium content indicates that the structure of Si–O–Si is possibly destroyed in local regions and more Si–O–Ti linkages are produced [28]. This is evidenced by the fact that the intensity of the 960 cm^{-1} band becomes stronger. Broad absorption at 650 cm^{-1} corresponding to Ti–O–Ti bonds is clearly observed in the ST1 sample, suggesting the formation of crystalline titania. This observation reveals that the environment of the Ti sites changes with the increase in titanium content and significant formation of anatase crystals occurs with a titanium content of higher than 50 mol%, agreeing well with the results obtained by XRD studies.

The linear variation of the 960 cm^{-1} band intensity is associated with titanium incorporation into the amorphous silica network in tetrahedral positions. A comparison of the

deconvoluted area of the band at around 960 cm^{-1} assigned to Si–O–Ti vibrations, and that of the Si–O–Si band observed at around 1210 cm^{-1} has previously been used as a means to quantify the dispersion of titanium in the silica matrix [29], as defined in Eq. 1:

$$R = \frac{S_{(Si-O-Ti)}}{S_{(Si-O-Si)}} \quad (1)$$

Figure 4 shows the comparison between surface and bulk Ti-concentration of SiO_2–TiO_2 mixed oxides with different Si/Ti ratios which were prepared from TTIP and TEOT, respectively. The relative abundance of Si–O–Ti connectivity, representing the surface Ti concentration, was calculated from Eq. 1. The bulk Ti concentration was expected on the basis of the chemical composition. The ST1 sample shows a lower Ti concentration on the surface (TTIP, 0.39; TEOT, 0.33) than in the bulk structure (1.0), indicating that some extension of hemolytic condensation may take place at high titanium content. The Ti–O–Ti bonds are therefore developed in the Ti-rich regions, resulting in the decrease in Si–O–Ti bonds as shown in Fig. 3. The explanation of this fact is based on the replacement of silicon by titanium in tetrahedrally coordinated positions at low Ti content, whereas octahedral Ti species are produced due to the formation of Ti–O–Ti bonds at higher Ti content [30].

In the case of samples ST5, ST10, and ST50, regardless of the influence of Ti precursors, the surface Ti concentration is always higher than the corresponding bulk Ti concentration. The present discussion shows that Ti is mainly found highly dispersed at the surface of the mixed oxides with low titanium content [31]. In addition, the mixed oxides prepared from TTIP always show a higher surface Ti concentration than those from TEOT. Apparently, compared with TEOT, TTIP is more easily dispersed in the sol–gel solution for preparing SiO_2–TiO_2 mixed oxides and encourages the formation of Si–O–Ti linkages.

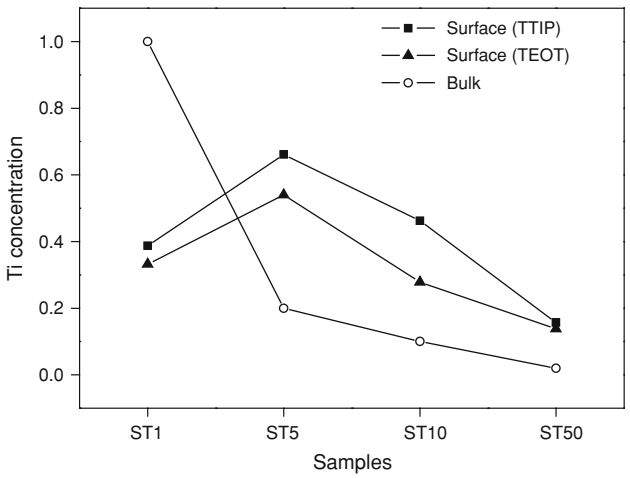

Fig. 4 Surface and bulk Ti concentration of SiO_2–TiO_2 mixed oxides prepared with different Ti precursors

The influence of titanium content and calcination temperature on the relative abundance of Si–O–Ti connectivity of SiO_2–TiO_2 mixed oxides has been studied and the results are shown in Table 2. The relative abundance of Si–O–Ti connectivity of the SiO_2–TiO_2 mixed oxides calcined at 550 °C varies with Si/Ti ratios and the maximum value (R) 0.66 is obtained in the case of the ST5 sample. The 960 cm^{-1} IR band is observed both in the raw SiO_2–TiO_2 xerogel and the resultant solids and indicates that Si–O–Ti bonds are not only present in the calcined samples but also in the starting xerogel. The value (R) of the raw xerogel is 0.38, revealing that Si–O–Ti bonds are formed during the sol–gel process. It should be noted that an R-value of 0.38 is obtained for the resultant solid after calcination at 250 °C, and this is the same as that of the raw xerogel. Therefore, we can conclude that calcination of the xerogel at a low temperature does not influence the Si–O–Ti connectivity.

As the calcination temperature increases from 300 to 500 °C, the value (R) increases slightly from 0.41 to 0.50. This can be rationalized in terms of the decomposition of residual organic groups during heat treatment which would result in the breaking and rearrangement of chemical bonds and additional Si–O–Ti linkages are therefore produced. The value (R) drops to 0.46 after calcination at 550 °C and then continuously decreases with the increase in

Table 2 The relative abundance of Si–O–Ti connectivity and acid site density of SiO_2–TiO_2 mixed oxides

Sample	Temperature (°C)	R[a]	Total acid amount[b] (mmol g^{-1})
ST50	550	0.16	0.09
ST10	–	0.38	–
	250	0.38	–
	300	0.41	–
	400	0.46	–
	450	0.47	–
	500	0.50	0.33
	550	0.46	0.27
	600	0.39	0.05
	650	0.21	0.01
ST5	550	0.66	0.52
ST1	550	0.39	0.38

[a] Relative abundance of Si–O–Ti connectivity estimated from the ratio of the peak areas for Si–O–Ti (930–939 cm^{-1}) and Si–O–Si (1205–1215 cm^{-1}) determined by deconvolution of the original FTIR spectra

[b] Acid site density of the SiO_2–TiO_2 samples assumed to be equal to the amount of desorbed ammonia in the temperature range 120–500 °C

calcination temperature. It is reported that SiO_2–TiO_2 materials become unstable at a temperature of 500 °C; with further calcination, the existing Si–O–Ti linkages would be broken and Si–O–Si and Ti–O–Ti bonds are therefore formed in the bulk structure [32]. Nevertheless, SiO_2–TiO_2 mixed oxides with higher thermal stability estimated from XRD data have been reported in previous studies [25, 28, 33].

X-ray diffraction is well known as one of the most powerful techniques for characterizing the structural properties of crystalline solids. However, it does not provide sufficient information on the inner structure of amorphous materials. It is evident that when the segregated TiO_2 is highly dispersed in the silica matrix (size < 5 nm), its diffraction lines are not able to be detected by XRD [32]. Since FTIR spectroscopy gives precise data associated with chemical bonds and can reflect changes in internal structure, it is expected to be useful for the characterization of the thermal stability of SiO_2–TiO_2 mixed oxides.

3.4 Pyrolysis Process of Xerogels

FTIR measurements provide useful information on Si–O–Ti linkages of SiO_2–TiO_2 mixed oxides, which is helpful in probing into the evolution of the solid structure during heat treatment. Figure 5 shows typical TG and differential thermal analysis (DTA) curves of the SiO_2–TiO_2 xerogel (Si/Ti = 10). According to the results obtained by FTIR spectroscopy, the TG curve can be carefully divided into three stages in terms of physical and chemical processes that are occurring. The TG curve indicates an initial weight loss of 22.68 % between room temperature and 110 °C, corresponding to the release of physisorbed water and alcohols trapped in the porous texture [18]. The DTA curve, correspondingly, exhibits a strong endothermic peak at approximately 65 °C.

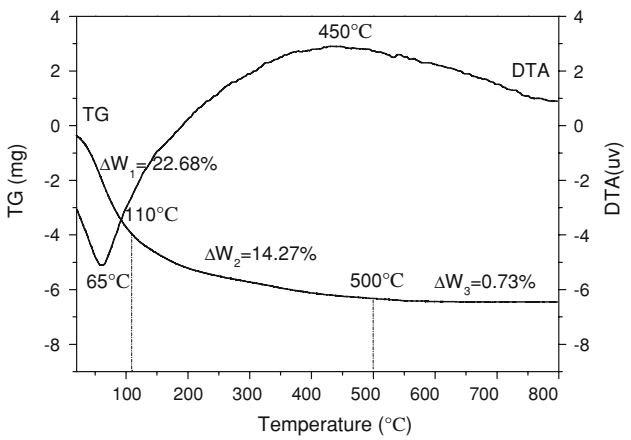

Fig. 5 TG and DTA curves of SiO_2–TiO_2 xerogel (Si/Ti = 10)

It is known that a large amount of hydroxyl groups still stay on the surfaces of sol–gel prepared SiO_2–TiO_2 materials, which gradually eliminate hydroxyl groups and become denser in structure upon heating [5, 34]. Despite the removal of structural hydroxyl groups, the decomposition of organic residues is also considered to occur in the temperature range from 110 to 500 °C. There is a further weight loss of 14.27% in the TG curve and the DTA curve shows a wide exothermal peak at around 450 °C. Since no variation of Si–O–Ti structural units is observed by FTIR spectroscopy after calcination at 250 °C, we can assume that the remaining organic groups in the bulk structure cannot be destroyed at low heating temperature; however, only structural hydroxyls are removed in the form of water. The Si–O–Ti linkages are therefore steadily enhanced with increasing calcination temperature, which can be attributed to the rearrangement of chemical bonds during the decomposition of organic residues [31].

The TG curve indicates a slight weight loss of 0.73% between 500 and 800 °C, which is assigned to removal of structural hydroxyls from the structure. The existing Si–O–Ti bonds would be broken at this stage, leading to the formation of Ti–O–Ti structural units but having no relationship to weight loss. It has been reported that titanium sites were associated with –OH terminal groups after calcination at temperatures up to 500 °C but were much reduced or completely removed after calcination at 750 °C [35].

3.5 Evolution of Titanium Coordination

3.5.1 UV–Vis Analysis

Figure 6 shows the UV–Vis spectra of pure silica and SiO_2–TiO_2 mixed oxides. Pure silica shows no pronounced absorption between 200 and 500 nm. However, a strong absorption signal is seen at 215 nm in SiO_2–TiO_2 mixed oxides. With increasing titanium content, the UV absorption edge is shifted to higher wavelengths, revealing growing coordination numbers of titanium [36]. In particular, the ST10 sample exhibits a significant band centered at 215 nm, indicating a higher proportion of Ti species with tetrahedral coordination in the polymeric SiO_2–TiO_2 network. In contrast to the ST10 sample, continuous absorption is observed between 215 and 260 nm in the ST5 sample. However, the ST1 sample shows a wide band in the region 215–320 nm. These results indicate that different Ti environments coexist in this material. Besides tetrahedrally coordinated Ti atoms, other Ti configurations must be present, including some assembly of Ti–O–Ti that is characteristic of a band at 320 nm. Regardless of the conclusions derived from the XRD and FTIR spectroscopy, these results show that the environment of the Ti sites in

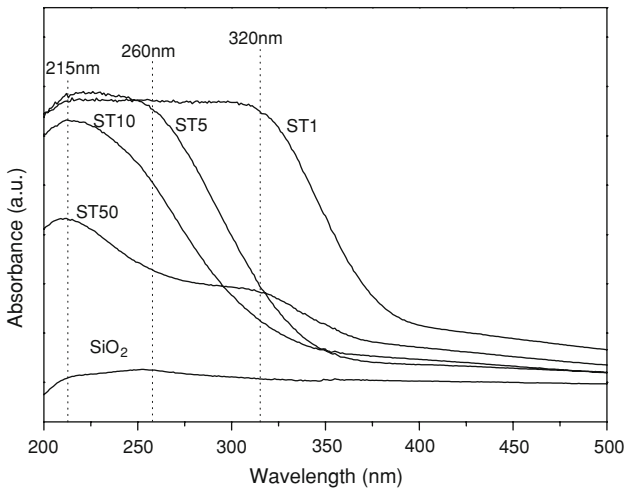

Fig. 6 UV–Vis spectra of pure silica and SiO_2–TiO_2 mixed oxides

the amorphous cogel changes gradually with the increase in titanium content during synthesis, leading to some of the Ti atoms being in octahedral positions [3, 37, 38].

3.5.2 XPS Analysis

It has been reported that the BE of the Ti 2p3/2 peak in amorphous SiO_2–TiO_2 sol–gel formed materials varies with titanium content [2, 19, 39]. The shift in BE can be explained by the increase in interatomic potential due to a decrease in the coordination number of Ti atoms, indicating the insertion of Ti^{4+} cations into the tetrahedral sites of the silica matrix [1]. The BE of pure titania is known to be 458.5 eV [2]. In the present case, the BE of the Ti 2p3/2 peak is 459.8 eV for the ST10 sample (not shown here). The upward shift of the Ti 2p3/2 value confirms the formation of Si–O–Ti linkages, which can significantly increase the effective positive charge on Ti species in SiO_2–TiO_2 mixed oxides [16, 17]. This fact gives further evidence that tetrahedral Ti(IV) species is abundantly formed in SiO_2–TiO_2 mixed oxides with a Si/Ti ratio of 10.

3.6 Surface Acidic Properties

3.6.1 Pyridine-FTIR Measurements

The nature of acidic sites (Brønsted and Lewis) has been determined by pyridine-FTIR. FTIR spectra of pyridine adsorbed on pure silica and SiO_2–TiO_2 mixed oxides are shown in Fig. 7a. According to previous studies, the band at 1540 cm^{-1} can be attributed to the vibrational modes of Brønsted coordinated pyridine, whereas the band at 1480 cm^{-1} is associated simultaneously with both Brønsted and Lewis acid sites. The band at 1445 cm^{-1} corresponds to vibration of pyridine chemisorbed on Lewis acid sites [40].

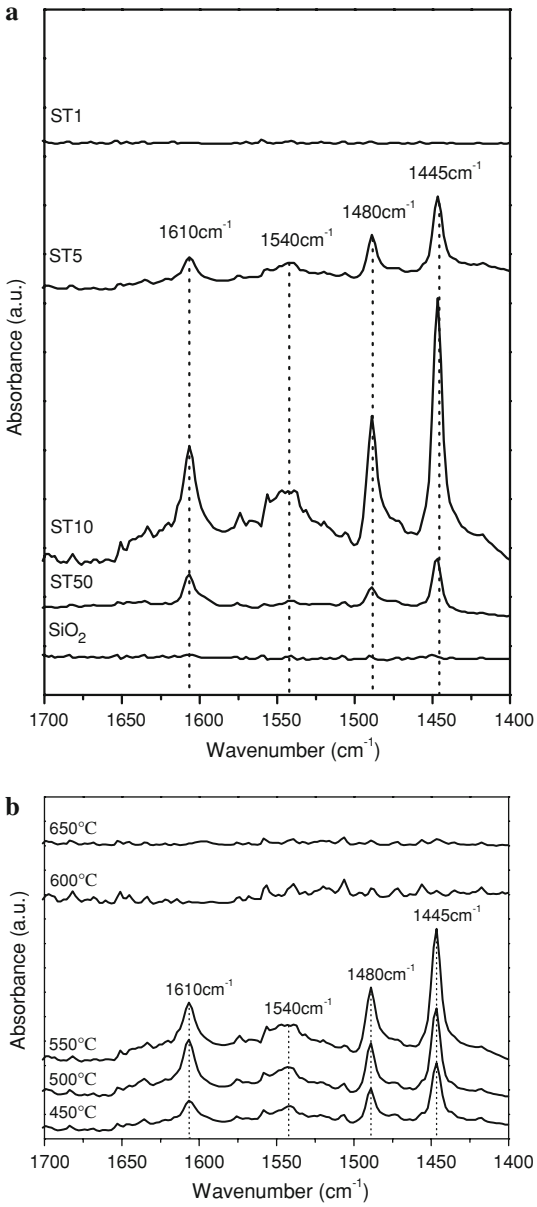

Fig. 7 FTIR spectra of pyridine adsorption on (**a**) pure silica and SiO_2–TiO_2 mixed oxides calcined at 550 °C; (**b**) SiO_2–TiO_2 xerogel (Si/Ti = 10) after calcination at various temperatures

Pure silica shows no vibrational bands. The samples ST50, ST10, and ST5 exhibit four bands at 1610, 1540, 1480, and 1445 cm^{-1}, indicating that the introduction of Ti species into silica leads to the formation of both Brønsted and Lewis acid sites [41]. In particular, the ST10 sample appears to possess the maximum of both Brønsted and Lewis acid sites in terms of the intensity of IR bands. Nevertheless, neither Brønsted nor Lewis acid sites are detected in the ST1 sample. Tanabe's model predicts that Lewis acidity is generated by the presence of an excess of positive charge while an excess of negative charge is responsible for Brønsted acidity [42]. The materials are

homogeneous as expected when the sol–gel method is used under high control of the preparation conditions to form SiO_2–TiO_2 mixed oxides. For the ST1 sample with equal molar compositions, there are theoretically no Si- or Ti-rich regions in the bulk structure and it is free from charge imbalance in Si–O–Ti bonds. As a result, no acidic sites are generated in the mixed oxide system.

Figure 7b shows FTIR spectra of pyridine adsorbed on the mixed oxides with Si/Ti = 10 calcined at various temperatures. The mixed oxides calcined at 450–550 °C show four obvious bands at 1610, 1540, 1480, and 1445 cm^{-1}. After calcination at 600 °C, a sharp decrease in these bands is observed. It is noted that no apparent absorbance is seen in the FTIR spectra of the mixed oxide calcined at 650 °C. These results reveal that the population of surface acidic sites also relies on the thermal treatment performed on raw xerogels.

Over the past few decades, several hypotheses have been proposed to explain the origin of the development of acidic properties in SiO_2–TiO_2 mixed oxides [42–44]. Although none are completely applicable owing to the surface complexity, it is widely accepted that Brønsted acidity is associated with the Si–O–Ti linkage [15, 19, 32]. Regardless of the contribution to Lewis acidity, surface hydroxyls are known to play a key role in the development of Brønsted acid sites. The bridging Si–O(H)–Ti hydroxyls have been supposed to be Brønsted acid sites. It is clearly shown that the breaking of Si–O–Ti linkages begins to occur at about 500 °C during heat treatment as indicated by FTIR spectroscopy. In addition, the removal of structural hydroxyls is also found to take place in this process. Accordingly, it can be confirmed that the decrease in Brønsted and Lewis acid sites is strongly related to the breaking of Si–O–Ti bonds as well as the removal of structural hydroxyls.

3.6.2 Ammonia TPD Measurements

Pyridine-FTIR distinguishes between adsorbed molecules bonded in a coordinated fashion on Lewis and Brønsted acid sites. However, quantification is more difficult [17]. Ammonia TPD is a well-known method for the determination of surface acidity of solid heterogeneous catalysts as well as acid strength. The acid site densities of pure silica and SiO_2–TiO_2 mixed oxides are listed in Table 2. No NH_3-release peak obtained in the TPD profiles (not shown here) for pure silica indicates the absence of any acid sites in the material, correlating well with the results obtained by pyridine-FTIR. A very low peak is observed at around 190 °C in the ST50 sample. The amount of NH_3 desorbed is 0.09 mmol g^{-1}.

TPD profiles of samples ST10, ST5, and ST1 are similar and consist of one broad peak which has a long tail, finally reaching the baseline at 500 °C. The maxima of the ammonia desorption peaks are centered at a low temperature approximately 190 °C. By considering the related values of temperature corresponding to peak NH_3 desorption, the strength of the acid sites remains almost constant. Furthermore, it is suggested that the surface acidity originates from the presence of weak acid sites. The total amount of NH_3 desorbed from the ST10 and ST1 samples is 0.27 and 0.38 mmol g^{-1}, respectively. The largest amount of desorbed NH_3 (0.52 mmol g^{-1}) is obtained in the ST5 sample.

These results clearly show that the presence of weak acid sites is significant in the material with Si/Ti = 1. This seems to conflict with the results from pyridine-FTIR, that neither Brønsted nor Lewis acid sites are observed. Nevertheless, SiO_2–TiO_2 mixed oxide with Si/Ti = 1 has been reported to have significant acid sites everywhere. Contescu et al. [15] showed that, since the pyridine-FTIR and ammonia TPD experiments are generally performed under different conditions using different probe molecules, when the two methods are compared, the information obtained should be considered with caution. In addition, it is evident that adsorption of NH_3 on non-Brønsted sites may be stronger than on Brønsted sites and the desorption temperature is heavily dependent on the conditions used for the experiment. Gorte [45] proposed that, when using ammonia TPD to determine the acidity of materials, the results should be treated with caution. Other experiments are in progress to gain further understanding of this particular observation on the surface acidity of the SiO_2–TiO_2 mixed oxide with Si/Ti = 1.

The acid site densities of SiO_2–TiO_2 mixed oxides with Si/Ti = 10 calcined at various temperatures are also listed in Table 2. To avoid the influence of organic residues, mixed oxides obtained between 500 and 650 °C were selected. The mixed oxide shows a continuous decrease in the amount of NH_3 desorbed with the increase in calcination temperature. The amount of NH_3 desorbed on the mixed oxide calcinated at 500 °C is 0.33 mmol g^{-1}. After calcination at 650 °C, only 0.01 mmol g^{-1} is observed for the amount of NH_3 desorbed on the mixed oxide, indicating a very low acid site density.

Comparing the results in Table 2 with those obtained from pyridine-FTIR as shown in Fig. 7b, we can conclude that the independent techniques used are in good agreement and they are reliable for estimating the changes in surface acidic sites with increasing temperature. It can be seen from Table 2 that there is a continuous decrease in the relative abundance of Si–O–Ti connectivity when calcination temperature rises from 500 to 650 °C. According to the results of TGA, this decline in the amount of NH_3 desorbed on SiO_2–TiO_2 mixed oxide with increasing calcination temperature can be attributed to the breaking of

Si–O–Ti linkages and the removal of structural hydroxyls. Taking into account the influence of both titanium content and calcination temperature, it is clearly seen that there is a positive correlation between the abundance of Si–O–Ti connectivity and the acid site density of SiO_2–TiO_2 mixed oxides.

3.7 Threshold of Tetrahedral Ti(IV) species

Beck et al. [24], Nur [46], and Mul et al. [47] have evidenced that isolated Ti(IV) in tetrahedral form in SiO_2–TiO_2 mixed oxides is the most active species in the epoxidation reaction. Ding et al. [37] found that the highly dispersed Ti(IV) sites are also good catalytic centers for selective oxidation of organic compounds. It emerges from the mechanism of reaction that characterization of the acidity is crucial for understanding the nature of the active sites. However, due to the remarkable influence of preparation conditions, there is no general agreement on the maximum titanium content that can be effectively incorporated into the silica matrix of sol–gel SiO_2–TiO_2 formed materials.

Our results indicate that a higher proportion of tetrahedral Ti(IV) species is detected in the resulting SiO_2–TiO_2 mixed oxides with a Si/Ti ratio about 10 after calcination at 550 °C. It is interesting to compare this result with that of other investigations. From the results of EXAFS and ESR measurements, Kanai et al. [11] proposed that Ti sites in <10 mol% TiO_2–SiO_2 mixed oxides (Si/Ti = 10) were of tetrahedral configuration, while those with higher Ti content were of octahedral configuration. Klein et al. [7] reported that isolated titania dominate the Ti distribution in the SiO_2–TiO_2 mixed oxides with Ti contents from 0 to 9 mol% (Si/Ti = 10.1), which was evidenced by UV–Vis spectroscopy. Jung et al. [19] showed that in the case of 10 mol% SiO_2–TiO_2 (Si/Ti = 11.1), Ti atoms were highly dispersed in the silica network. Using XRD, XPS, and XANES, Kim and Lee [48] observed that the surface Ti(IV) species of TiO_2/SiO_2 catalysts was directly responsible for the selective synthesis of methylphenylcarbonate (MPC). The amount of the surface Ti(IV) species measured by XPS was found to increase with Ti loading and was saturated above 10 wt% (Si/Ti = 12.0). Using a combination of spectroscopic techniques, Wallidge et al. [5] and Rigden et al. [49] demonstrated that, for $(TiO_2)_x(SiO_2)_{1-x}$ samples with $x = 0.08$ (Si/Ti = 11.5), all titanium atoms were tetrahedrally coordinated.

These results have shown that there is in fact a reference limit to the proportion of Ti atoms that can enter into silicon sites of SiO_2–TiO_2 mixed oxides by substitution. Unlike the fixed value for the Ti-substituted zeolites, it varies from 10 to 12 with different preparation conditions. In conclusion, to maximize the tetrahedral Ti(IV) species of sol–gel derived SiO_2–TiO_2 materials, several preparation parameters including Ti precursors, content, and calcination temperature should be carefully considered.

4 Conclusions

Sol-gel formed SiO_2–TiO_2 mixed oxides are largely amorphous and characterized by Ti enrichment on surfaces with low titanium content; however, the addition of titanium greater than 50 mol% into the SiO_2 matrix leads to significant phase separation of crystalline anatase.

Si–O–Ti linkages are initially formed in the sol–gel process and are further enhanced by rearrangement of chemical bonds during heat treatment up to 500 °C, but are then reduced with further calcination. With Si/Ti ratios above 10, the Ti atoms are tetrahedrally coordinated and gradually enter into octahedral positions in the silica matrix with further increase in titanium content.

A positive relationship has been established between the relative abundance of Si–O–Ti connectivity and the total acid amount, and the highest density of acid sites is observed at a Si/Ti ratio of five for the mixed oxide. High-temperature treatment can break Si–O–Ti linkages and eliminate hydroxyl groups, resulting in a decrease in acid site density.

Acknowledgments We are grateful for the financial support from the National Basic Research Program of China (2005CB221204) and the National Natural Science Foundation of China (20606022).

References

1. Gao X, Wachs IE (1999) Catal Today 51:233
2. Pabón E, Retuert J, Quijada R, Zarate A (2004) Microporous Mesoporous Mater 67:195
3. Davis RJ, Liu Z (1997) Chem Mater 9:2311
4. Dutoit DCM, Schneider M, Hutter R, Baiker A (1996) J Catal 161:651
5. Wallidge GW, Anderson R, Mountjoy G, Pickup DM, Gunawidjaja P, Newport RJ, Smith ME (2004) J Mater Sci 39:6743
6. Grunwaldt JD, Beck C, Stark W, Hagen A, Baiker A (2002) Phys Chem Chem Phys 4:3514
7. Klein S, Weckhuysen BM, Martens JA, Maier WF, Jacobs PA (1996) J Catal 163:489
8. Walters JK, Rigden JS, Dirken PJ, Smith ME, Howells WS, Newport RJ (1997) Chem Phys Lett 264:539
9. Moretti G, Salvi AM, Guascito MR, Langerame F (2004) Surf Interf Anal 36:1402
10. Jung M (2001) Int J Inorg Mater 3:471
11. Kanai H, Shono M, Hamada K, Imamura S (2001) J Mole Catal A 172:25
12. Li C (2003) J Catal 216:203
13. Dutoit DCM, Göbel U, Schneider M, Baiker A (1996) J Catal 164:433
14. Hutter R, Mallat T, Peterhans A, Baiker A (1999) J Mole Catal A 138:241

15. Contescu C, Popa VT, Miller JB, Ko EI, Schwarz JA (1995) J Catal 157:244
16. Wang SP, Ma XB, Guo HL, Gong JL, Yang X, Xu GH (2004) J Mole Catal A 214:273
17. Samantaray SK, Parida K (2001) Appl Catal A 220:9
18. Samantaray SK, Parida K (2005) Appl Catal B 57:83
19. Jung SM, Dupont O, Grange P (2001) Appl Catal A 208:393
20. López T, Bosch P, Tzompantzi F, Gómez R, Navarrete J, lópez-Salinas E, Llanos ME (2000) Appl Catal A 197:107
21. Doolin PK, Alerasool S, Zalewski DJ, Hoffman JF (1994) Catal Lett 25:209
22. Millini R, Massara EP, Perego G, Bellussi G (1992) J Catal 137:497
23. Bonelli B, Cozzolino M, Tesser R, Serio MD, Piumetti M, Garrone E, Santacesaria E (2007) J Catal 246:293
24. Beck C, Mallat T, Bürgi T, Baiker A (2001) J Catal 204:428
25. Serrano DP, Uguina MA, Ovejero G, Grieken VR, Camacho M (1996) Microporous Mater 7:309
26. Sing KSW, Rouquerol J (1997) In: Ertl G, Knözinger H, Weitkamp J (eds) Handbook of heterogeneous catalysis, vol 2. Wiley-VCH, Weinheim, p 431
27. Song CF, Lü MK, Yang P, Xu D, Yuan DR (2002) Thin Solid Films 413:155
28. Shao PL, Mauritz KA, Moore RB (1995) Chem Mater 7:192
29. Müller CA, Maciejewski M, Mallat T, Baiker A (1999) J Catal 184:280
30. Uguina MA, Serrano DP, Ovejero G, Grieken VR, Camacho M (1995) Appl Catal A 124:391
31. Lee BS, Kang DJ, Kim SG (2003) J Mater Sci 38:3545
32. Samantaray SK, Parida K (2001) Appl Catal A 211:175
33. Izutsu H, Nair PK, Maeda K, Kiyozumi Y, Mizukami F (1997) Mater Res Bull 32:1303
34. Jiang X, Wang T, Wang YW (2004) Colloids Surf A 234:9
35. Yang J, Ferreira JMF, Weng WJ, Tang Y (1997) J Colloid Interf Sci 195:59
36. Samantaray SK, Parida K (2003) React Kinet Catal Lett 78:381
37. Ding Z, Zhu HY, Greenfield PF, Lu GQ (2001) J Colloid Interf Sci 238:267
38. Xie C, Xu ZL, Yang QJ, Xue BY, Du YG, Zhang JH (2004) Mater Sci Eng B 112:34
39. Garbassi F, Balducci L (2001) Microporous Mesoporous Mater 47:51
40. Rajagopal S, Marzari JA, Miranda R (1995) J Catal 151:192
41. Rahman A, Lemay G, Adnot A, Kaliaguine S (1988) J Catal 112:453
42. Tanabe K, Misono M, Ono Y, Hattori H (1989) New solid acids and bases: their catalytic properties. Kodansha-Elsevier, Tokyo, p 185
43. Nakabayashi H, Kakuta N, Ueno A (1991) Bull Chem Soc Jpn 64:2428
44. Kataoka T, Dumesic JA (1988) J Catal 112:66
45. Gorte RJ (1999) Catal Lett 62:1
46. Nur H (2006) Mater Sci Eng B 133:49
47. Mul G, Zwijnenburg A, Linden BVD, Makkee M, Moulijn JA (2001) J Catal 201:128
48. Kim WB, Lee JS (1999) J Catal 185:307
49. Rigden JS, Walters JK, Dirken PJ, Smith ME, Bushnell-Wye G, Howells WS, Newport RJ (1997) J Phys: Condens Matter 9:4001